UCSF

UC San Francisco Previously Published Works

Title

Preliminary Diffusive Clearance of Silicon Nanopore Membranes in a Parallel Plate Configuration for Renal Replacement Therapy

Permalink

https://escholarship.org/uc/item/9gk2c8mp

Journal

ASAIO Journal, 62(2)

ISSN

1058-2916

Authors

Kim, Steven

Heller, James

Iqbal, Zohora

et al.

Publication Date

2016-03-01

DOI

10.1097/mat.0000000000000311

Peer reviewed

eScholarship.org Powered by the California Digital Library
University of California

Author Manuscript

Author Manuscript

Author Manuscript

Author Manuscript

HHS Public Access

Author manuscript

*ASAIO J*. Author manuscript; available in PMC 2017 March 01.

Published in final edited form as:

*ASAIO J*. 2016 ; 62(2): 169–175. doi:10.1097/MAT.0000000000000311.

# Preliminary Diffusive Clearance of Silicon Nanopore Membranes in a Parallel Plate Configuration for Renal Replacement Therapy

**Steven Kim**[1,2], **James Heller**[1], **Zohora Iqbal**[1], **Rishi Kant**[1], **Eun Jung Kim**[1], **Jeremy Durack**[3,+], **Maythem Saeed**[3], **Loi Do**[3], **Steven Hetts**[3], **Mark Wilson**[3], **Paul Brakeman**[4], **William H. Fissell**[5], and **Shuvo Roy**[1,*]

[1]Department of Bioengineering and Therapeutic Sciences, University of California, San Francisco, QB3/Byers Hall, Room 203A, MC 2520, 1700 4TH Street, San Francisco, California 94158, Phone: (415) 514-9666

[2]Division of Nephrology University of California, San Francisco, 521 Parnassus Ave, San Francisco, California 94143, Phone: (415) 476-2172

[3]Department of Radiology and Biomedical Imaging, University of California, San Francisco, UCSF Imaging Center at China Basin, 185 Berry Street, Suite 190, Lobby 6, San Francisco, California 94107, Phone: (415) 353-4500

[4]Division of Pediatric Nephrology University of California, San Francisco, 533 Parnassus Ave, UC Hall, San Francisco, California, 94143, Phone: (415) 476-2423

[5]Division of Nephrology and Hypertension, Vanderbilt University Medical Center, 1211 Medical Center Drive, Nashville, Tennessee 37232, Phone: (615) 322-4794

## Abstract

Silicon nanopore membranes (SNM) with compact geometry and uniform pore size distribution have demonstrated a remarkable capacity for hemofiltration. These advantages could potentially be used for hemodialysis. Here we present an initial evaluation of the SNM's mechanical robustness, diffusive clearance, and hemocompatibility in a parallel plate configuration. Mechanical robustness of the SNM was demonstrated by exposing membranes to high flows (200ml/min) and pressures (1,448mmHg). Diffusive clearance was performed in an albumin solution and whole blood with blood and dialysate flow rates of 25ml/min. Hemocompatibility was evaluated using scanning electron microscopy and immunohistochemistry after 4-hours in an extra-corporeal porcine model. The pressure drop across the flow cell was 4.6mmHg at 200ml/min. Mechanical testing showed that SNM could withstand up to 775.7mmHg without fracture. Urea clearance did not show an appreciable decline in blood versus albumin solution. Extra-corporeal studies showed blood was successfully driven via the arterial-venous pressure differential without thrombus formation. Bare silicon showed increased cell adhesion with a 4.1 fold increase and 1.8 fold increase over polyethylene-glycol (PEG)-coated surfaces for tissue plasminogen factor (t-PA) and platelet adhesion (CD-41), respectively. These initial results

[*]Corresponding Author: Steven Kim, MD (steven.kim@uscf.edu) .

[+]*now at* Department of Radiology, Memorial Sloan Kettering Cancer Center, 1275 York Avenue, Suite H-118, New York, New York 10065, Phone: (212) 639-4898

Author Manuscript Author Manuscript Author Manuscript Author Manuscript

warrant further design and development of a fully scaled SNM-based parallel plate dialyzer for renal replacement therapy.

**Keywords**

MEMS; microfabrication; portable hemodialysis; parallel plate dialyzer

## INTRODUCTION

End Stage Renal Disease (ESRD) remains a major public health problem in the United States – afflicting over 615,000 people with nearly 116,000 new patients initiating treatment each year.[1] Due to the shortfall in organ availability, the majority of ESRD patients in the United States must undergo in-center, 3-4 hour, thrice weekly hemodialysis. Currently, high-flux hollow-fiber dialyzers have usurped all other membrane technologies given their large surface area, favorable transport, and low manufacturing costs. However, polymer hollow-fiber membranes have several inherent limitations that hinder further advancements and have resulted in stagnant patient outcomes. First, significant blood-to-dialysate flow mismatch can occur due to uneven blood flow distribution and dialysate channeling from uneven fiber packing.[2] Second, polymer membranes have inherent biocompatibility problems due to clotting and activation of platelet, leukocyte, and complement, which limits long-term continuous use.[3] Third, the high internal resistance of hollow-fiber dialyzers requires an external blood pump that also results in deleterious cell activation and micro-bubble formation.[4] Finally, hollow-fiber polymer membranes have wide pore size distributions, tortuous flow paths, and roughly circular-shaped cross-sectional pore geometries that limit their selectivity and permeability compared to slit pore geometries.[5]

Parallel plate dialyzers, on the other hand, allow for the potential for uniform blood and dialysate flow across a flat surface. The internal flow resistance with a large width to height ratio is dependent upon the viscosity, path length, blood flow rate and width to height dimensions[6]. Therefore, by manipulating the height and width of the flat plate channel the internal resistance can be significantly reduced, negating the need for an external blood pump. These attributes popularized the flat plate hemodialyzer design [7-10] and the Kiil dialyzer dominated the market in the 1960's[11]. However, due to deficiencies in membrane technology at the time and advantages of hollow-fiber membranes, the flat plate design was supplanted. Today, however, microelectromechanical systems (MEMS) technology enables cost-effective production of flat sheets of silicon-based membranes with unprecedented control of pore size and geometry.[12] Therefore, there is increased interest in combining new and innovative silicon-based membrane technology with the advantageous design elements of the parallel plate dialyzer.

Recently, *Ahmadi et al.* and *Johnson et. al.* used flat MEMS based ultrathin porous nanocrystalline silicon membranes from SiMPore (N.Y. USA) to investigate in vitro clearance of small molecules and hemocompatibility using a single parallel plate configuration.[13, 14] These flat membranes had average circular pore sizes of 5 and 20nm with a membrane thickness of 30 nm. They were able to show clearance of small solutes

Author Manuscript Author Manuscript Author Manuscript Author Manuscript

over a total membrane area of 3 $mm^2$. The main limitation was fragility of the membrane requiring testing at very low flow rates (82.5 μl/min) and static dialysate to avoid mechanical failure.

Our group has previously pioneered a novel and robust silicon nanopore membranes (SNM) based on MEMS fabrication techniques for use in a fully implantable bioartificial kidney. The SNM have been extensively evaluated for their ability to function as a hemofilter.[5, 12, 15] The slit-pore design allows for an order of magnitude higher hydraulic permeability than commercially available hollow-fiber membranes.[15] Furthermore, the uniform pore size of SNM allows for extremely selective size based filtration with strict molecular weight cut-offs.

To exploit the advantages of a parallel plate design, we have investigated the ability of SNM to perform diffusive clearance. In this initial evaluation, we first examined the mechanical robustness of SNM under supra-physiologic conditions. Next, diffusive clearance of a scaled-down array of SNM in a parallel plate channel was tested. We compared transport in an albumin solution versus whole blood to evaluate any decline in membrane transport in a blood environment. Finally, we tested pumpless blood flow in an extra-corporeal parallel plate circuit to assess thrombosis and surface cell adhesion. By characterizing key parameters necessary to evaluate a SNM-based parallel plate dialyzer, our intent is to lay the foundation for future large-scale devices.

## MATERIALS AND METHODS

### Membrane Fabrications

Silicon nanopore membranes were fabricated using previously described microfabrication techniques.[12] Membranes were composed of a 300 nm polysilicon layer with an array of rectangular pore slits measuring 4.5 μm × 10 nm. The structural support layer was composed of <100>-oriented, n-type crystalline silicon with 400 μm thickness. Wafers were diced into 10 × 10 mm chips with an effective membrane area of 0.216 $cm^2$. The hydraulic permeability of SNM were tested to verify membrane integrity and determine pore size[12].

### Surface Modification

Polyethylene glycol (PEG) surface modification was performed on polysilicon surfaces.[16] Briefly, SNM were treated with a 3:1 sulfuric acid to hydrogen peroxide (Piranha) solution to functionalize the polysilicon surface with hydroxyl groups. Membranes were submersed in 25 ml of toluene and 285 μL of PEG-silane (Sigma Aldrich, St. Louis MO) at 70 °C for 2 hours. Surface modified membranes were then rinsed at 10 minutes intervals (3×) with toluene (Gelest Morrisville, PA), ethanol, and deionized water. Hydraulic permeability was retested following PEG coating to measure the pore size change after surface modification. SNM coating thickness was sub-5nm.

### Parallel Plate Array Flow Cell

A two-channel parallel plate flow cell capable of housing and testing multiple SNM chips exposed to blood flow was developed (Figure 1). It consisted of two titanium (grade 2

Author Manuscript Author Manuscript Author Manuscript Author Manuscript

commercially pure) inlet and outlet ports. These were positioned perpendicular to the plates for even fluid distribution. The main body of the device consisted of a stacked set of parallel plates (titanium, grade 2 commercially pure), with alternating channels for blood (internal part of each plate) and dialysate flow (in the interfaces between the plates). A single internal blood channel was 60mm × 30mm × 2.4 mm (l × w × h) and defined by: a top plate (solid silicon sheet, 6 × 3 cm), and bottom plate (8 SNM or solid silicon mounted into the titanium holder with polydimethylsiloxane). The plates were sealed together using high purity silicone gaskets and screws to prevent leakage. Dialysate flow was split into two inlet ports and two outlet ports on the center plate. Uniform dialysate flow in a counter-current direction was achieved via an array of multiple 1mm diameter channels across the width of the dialysate plate. The dialysate channel was defined by the height of the compressed gasket (0.4 mm) with length of 60mm and width of 30mm. The titanium end caps were machined by Hayes Manufacturing Services (Sunnyvale, CA) and the remaining components were machined in our lab. *SolidWorks* software (DS Solidworks, Waltham, Massachusetts) was used to design all components.

## Mechanical Testing

Mechanical robustness of SNM were tested at a range of pressures (1448mmHg) using a syringe pump (KD410, KDS Scientific, Holliston, MA) and pressure gauge (DPI 104 30psi, GE Druck, Leicester, UK). Pressure was ramped at 25.9 mmHg until membrane rupture or 1448 mmHg was reached (n = 11).

Static and dynamic leak testing of the parallel plate array was conducted over a range of differential pressures (0-200mmHg). Pressure drop across the array (inlet to outlet) was measured over a range of flow rates (0-200 ml/min). A Masterflex L/S Digital Drive Peristaltic Pump, (MK-07551-00, Cole Parmer, Vernon Hills, IL) was used to drive flow and pressure in the system was monitored using two pressure gauges (DPI 104 10psi, GE Druck, Leicester, UK).

## Parallel Plate Array Diffusive Clearance

Eight PEG coated SNM chips were mounted onto the blood channel plate of the flow cell. The average pore size of the SNM was 6.5 nm ± 0.6 and the combined effective membrane surface area was 1.73 $cm^2$. The albumin solution consisted of creatinine 10 mg/dL (Acros Organics, Geel, Belgium), 88 mg/dL blood urea nitrogen (Fisher Scientific, Waltham, MA), 5mg/dL phosphorus (Sigma, St. Louis, MO), and 3 g/dL albumin (Sigma, St. Louis, MO) in Millipore water (Millipore, Billerica, MA) in a volume of 13ml. Whole blood diffusion experiments were conducted using 30ml of heparinized (20units/ml) bovine whole blood (Lampire Biological Laboratories, Pipersville, PA). The albumin solution or whole blood was recirculated and 1L of dialysate (140mEq of NaCl) was recirculated in a counter-current fashion (Figure 1). The flow rates for both solutions were set to 25 ml/min using a peristaltic pump to maintain pressures of <30 mmHg and limit transmembrane pressures. The system was preconditioned with the solutions for 30 minutes. Samples of albumin solution or whole blood and dialysate were collected at 0, 2, and 5 hours (n=3). The whole blood experiments were also conducted for 24 hours (n=2). The flow cell was disassembled and evaluated for thrombus formation, membrane fracture, or leaks. The concentrations of the different solutes

Author Manuscript Author Manuscript Author Manuscript Author Manuscript

were measured using an Avida 1800 Chemistry System (Siemens Medical, Erlangen, Germany) at San Francisco General Hospital (San Francisco, CA). Solute clearance (K) was calculated by fitting concentrations measured at serial time points an exponential decay function: $C(t)=C_i e^{-Kt/V}$, where C(t) was the concentration at time *t*, $C_i$ was the initial concentration, t was the time, and V was the volume.

## Extracorporeal Porcine Experiment

Pumpless blood flow characteristic in a parallel plate SNM array within an extracorporeal blood circuit was evaluated in a pig for four hours with University of California, San Francisco Institutional Animal Care and Use Committee approval. A ~20kg Yorkshire pig was anesthetized and systematic heparin anticoagulation therapy was delivered in bolus (200 IU/kg) followed by continuous infusion (125 IU/kg/hr). The renal artery and vein were cannulated using ultrasound and fluoroscopic guidance, with two single lumen catheters (Deltec Ventra Long-term Central Venous Catheters, Single-Lumen, 9FR, PN 21-2368-01, Smiths Medical, Dublin, OH). The inlet of the flow cell was attached to the arterial catheter and outlet was attached to the venous catheter, completing the extracorporeal arterio-venous circuit. Several minutes after the experiment began, a fluoroscopic contrast agent (Omnipaque 300, GE Healthcare, Little Chalfont, UK) was injected. Cine images were obtained during a 90-second dynamic infusion of contrast. Gross qualitative flow through the device was evaluated[17].

The extracorporeal circuit was run for a total of four hours uninterrupted. At the end of the experiment, with the device still attached, a second bolus of contrast agent was delivered and the device was re-imaged. The contrast front was again visualized flowing across the device. The arterial and venous catheters were then clamped and the device was disconnected from the extracorporeal circuit and drained. In order to prevent the remaining stagnant blood from coagulating, the cartridge was immediately cleared with heparinized saline until it ran clear. It was fully drained and then primed with a solution of 4% paraformaldehyde and deionized water. The device was carefully disassembled in order to examine the device for thrombus formation and leakage.

## Cell and Protein Adhesion Studies

**Scanning electron microscopy (SEM)—**The SNM were placed in a solution containing 2% glutaraldehyde (Electron Microscopy Sciences, Fort Washington, PA), 3% sucrose (Sigma-Aldrich, St. Louis, MO) and 0.1 M of phosphate buffered saline (PBS) at 4 °C and pH 7.4. After 1 h, the substrates were rinsed twice with PBS for 30 min at 4 °C and washed with distilled water for 5 minutes. Dehydration was achieved by placing the substrates in 50% ethanol for 15 minutes while increasing the concentration of ethanol to 60, 70, 80, 90 and finally 100%. Dehydrated samples were then mounted on aluminum stubs, sputter-coated with gold-palladium, and examined using SEM (Ultra55 FEGSEM, ZEISS, Peabody, MA).

**Immunohistochemistry (IHC)—**Platelet adhesion and activation was assessed using immunofluorescence staining for the platelet marker, CD41 (Abcam, Cambridge, MA), and blood clot marker, tissue plasminogen activator (t-PA, Abcam, Cambridge, MA). Platelets

Author Manuscript Author Manuscript Author Manuscript Author Manuscript

were fixed in 4% paraformaldehyde (Fisher Scientific, Waltham, MA) for 15 minutes followed by incubation in 1% bovine serum albumin for 30 minutes to block nonspecific binding. Platelets were double-labeled as follows: substrates were first incubated with primary antibodies (t-PA), diluted 1:50 in PBS for 60 minutes followed by Alexa Fluor 546 donkey anti-mouse antibody (Invitrogen, Carlsbad, CA) diluted 1:100 in PBS for 60 minutes. Finally the samples were incubated with anti-human CD41 fluorescein isothiocyanate labeled mouse monoclonal antibody diluted 1:300 in PBS for 60 min. Four images were acquired per replicate using a Nikon Eclipse Ti-E motorized inverted microscope (Nikon Instruments INC., Melville, NY) to obtain a total of 12 images per substrate. The fluorescent intensity of the images was quantified using *ImageJ* [18, 19, 20].

## RESULTS

### Mechanical Testing

All SNM withstood mechanical pressure testing greater than 775.7mmHg. Four out of eleven SNM failed with an average pressure of 910.2 ± 51.7 mHg and the remaining seven SNM remained intact up to 1448mmHg. The parallel plate array was tested at varying flow rates up to 200 ml/min without leakage of fluid out of the assembled device or between the individual parallel plates. The measured pressure drop across the flow cell at a flow rate of 200 ml/min was 4.6 mmHg.

### Diffusive Clearance of SNM Parallel Plate Array

The change in concentration using single-pass measurements was below the level of detection due to the high flow rate indicating that diffusive clearance was no longer dependent on flow rate. Recirculated albumin solution and whole blood concentrations of creatinine, urea and phosphorus followed an exponential decay function characteristic of diffusive clearance. The clearance (K) normalized to SNM surface area for albumin solution and whole blood experiments are shown in Table 1. The initial albumin concentration was 3.17 g/dL ± 0.05 and 5-hour albumin concentration was 3.13 g/dL ± 0.12. There was no significant reduction in albumin concentration ($p < 0.05$). Overall, heparinized bovine whole blood experiments showed maintenance of diffusive clearance similar to albumin solution. There was no evidence of clot formation during the 2 and 5 hour collection times. However, there was visible clot formation within the blood reservoir after 24 hours. Upon disassembly of the device, it was found there were no gross thrombi or membrane occlusion after 24 hours of continuous blood circulation.

### Porcine Extracorporeal Circuit

The preliminary extracorporeal circuit study demonstrated pumpless blood flow through the parallel plate array without complications. The pig tolerated the device well and did not exhibit deterioration of hemodynamic parameters or clinical status (Figure 2a). The fluoroscopy images obtained at the start and end of the 4-hour experiment showed no degradation in flow characteristics, with uniform blood flow across the parallel plates (Figure 2b). There was no evidence of thrombus formation in the cannulated vessels or catheter. Disassembly of the device showed no visible thrombi or debris within the flow cell.

Author Manuscript Author Manuscript Author Manuscript Author Manuscript

### Hemocompatibility Assessment

Following disassembly of the flow cell, the silicon was imaged by SEM. There was cell adhesion on blood-exposed surfaces for both uncoated silicon and PEG-coated silicon. However, there was visually less platelet and neutrophil adhesion on the surface of PEG-coated silicon compared to bare silicon (Figure 3). Representative images showing platelet adhesion and blood clots were visualized by immunofluorescence staining for CD41 and t-PA on uncoated silicon and PEG-coated silicon surfaces (Figure 4). Total fluorescent intensity was used to quantify the amount of staining on the surface. Bare silicon surfaces had a 4.1-fold increase in fluorescent intensity for t-PA and a 1.8-fold increase in fluorescent intensity for CD41 compared to PEG coated surfaces.

## DISCUSSION

As discussed previously, prior ultrathin silicon membranes have been limited due to their mechanical fragility.[13] Here we demonstrated the mechanical robustness of SNM by showing that the membranes can consistently withstand pressures beyond 775.7 mmHg, which is well beyond any physiologic pressure encountered clinically. Of note, four out of eleven membranes failed before reaching the system maximum 1448 mmHg indicating mechanical differences at these extreme pressures. We also tested the SNM at flow rates as high as 200 ml/min. These results demonstrate that SNM are able to handle a broad range of flow rates and transmembrane pressure gradients without concern for membrane integrity.

SNM within a parallel plate flow cell were able to dialyze small solutes, while maintaining selectivity for larger macromolecules. The clearance values are comparable to current commercial polymer hollow-fiber membranes at low blood flow rates (200 ml/min) when normalized to surface area (Table 2). This preliminary study also demonstrated the ability of the SNM parallel plate flow cell to function in a blood environment. The device was able to clear solutes in bovine whole blood for up to 24 hours without evidence of significant decline in diffusive transport. A potential wearable artificial kidney device that is used daily for 8 hours would require a minimum spKt/V of 0.34 per treatment (V=35L) to achieve a weekly stdKt/V of 2.0.[21] Based on the presented clearance values for the SNM we would require a total of 0.21 $m^2$ surface area. This would result in a device about the size of a coffee cup with ~25-30 stacked parallel plates each with 10 × 8 cm membrane area.

The extra-corporeal study showed effective blood flow using only the arterial-venous pressure differential in a heparinzed pig without evidence of major thrombus after four hours. After disassembly, there was no evidence of visual clot formation within the flow cell or on the silicon surfaces. This indicates that during the four-hour experiment we had adequate blood flow characteristics to limit gross thrombosis. Surface analysis of the silicon showed also minimal platelet and clot formation, however, microemboli was not evaluated and could lead to embolic disease. Nevertheless, this animal study showed the feasibility of an extracorporeal pumpless parallel plate system using silicon substrates for short-term use. Further, investigation is warranted for long-term studies especially looking at blood material interaction, flow optimization within a parallel plate system and microemboli formation.

Author Manuscript Author Manuscript Author Manuscript Author Manuscript

The sub-5nm PEG-coated silicon showed significantly decreased cell and platelet adhesion compared with uncoated silicon. These thin-film coatings are a critical component to SNM feasibility for continuous long-term blood contact as they limit biofouling while still maintaining pore patency. Further work is being pursued with longer-term studies as well as exploration of other polymer surface coatings with enhanced biocompatibility and stability.

The main barrier to improving diffusive transport of the SNM is the 400μm membrane thickness, which is due to the standard silicon wafer thicknesses used to fabricate the SNM. In contrast, hollow fiber membranes have thickness ranges of 40-50μm. Our group is currently working to develop the next generation of SNM with significantly thinner membranes comparable to commercial hollow fiber membranes. This could theoretically increase the diffusive clearance of the membranes several fold and comparable to the mass transfer-area cofficient (KoA) of modern hollow fiber dialyzers. However, reduction in the thickness of the membrane to improve diffusion must be weighed against the mechanical robustness of the membranes.

## CONCLUSIONS

This study represents a preliminary evaluation of flat sheets of SNM for diffusive clearance in a parallel plate system. These promising results show that comparable diffusive clearance to hollow-fiber membranes is feasible in a compact device. We have also demonstrated diffusive transport that was not hindered by blood contact for 24 hours. Furthermore, we showed pumpless blood flow in an extra-corporeal circuit without major thrombosis or significant surface fouling. However, significant challenges remain to translate these preliminary results into a fully scaled portable parallel plate hemodialyzer. Controlling blood and dialysate flow through multiple parallel plates without leaking is a non-trivial challenge. Blood flow optimization at the inlet and outlet, uniform flow across the parallel plates, vascular connections and mechanical shock are additional challenges that will further complicate a fully scaled device. Nevertheless, the promising results justify further SNM optimization for diffusion, scaled parallel plate hemodialyzer design, and further extra-corporeal blood compatibility studies.

## Supplementary Material

Refer to Web version on PubMed Central for supplementary material.

## ACKNOWLEDGEMENTS

The assistance of Charles Blaha, Illya Gordon, Torin Yeager, Peter Soler on various aspects of experimentation and discussion are appreciated. This work was supported by the American Society of Nephrology Ben J. Lipps Research Fellowship, National Institute of Biomedical Imaging and Bioengineering of the National Institutes of Health under Award Number R01 EB014315, Wildwood Foundation and the John and Marcia Goldman Foundation.

## REFERENCES

1. USRDS annual data report 2013. 2013.
2. Ronco C. Fluid mechanics and crossfiltration in hollow-fiber hemodialyzers. Hemodiafiltration. 2007; 158:34–49.

Author Manuscript Author Manuscript Author Manuscript Author Manuscript


3. Takemoto Y, Naganuma T, Yoshimura R. Biocompatibility of the dialysis membrane. Hemodiafiltration: a New Era. 2011; 168:139–145.
4. Daugirdas JT, Bernardo AA. Hemodialysis effect on platelet count and function and hemodialysis-associated thrombocytopenia. Kidney Int. 2012; 82(2):147–157. doi: 10.1038/ki.2012.130. [PubMed: 22592187]
5. Conlisk AT, Datta S, Fissell WH, Roy S. Biomolecular transport through hemofiltration membranes. Ann Biomed Eng. 2009; 37(4):722–736. doi: 10.1007/s10439-009-9642-0. [PubMed: 19184436]
6. Hoenich, N.; Woffindin, C.; Ward, M. Dialysers. In: Maher, J., editor. Replacement of Renal Function by Dialysis. 3rd ed.. Kluwer Academic Publishers; Netherlands: 1989. p. 144
7. Clark WR. Hemodialyzer membranes and configurations: A historical perspective. Semin Dial. 2000; 13(5):309–311. doi: 10.1046/j.1525-139x.2000.00081.x. [PubMed: 11014692]
8. Freeman RB, Roushey G, Hegadus V, Pabico RC, Cestero R. Clinical implications of fluid mechanics in parallel flow plate dialyzers. Clin Nephrol. 1974; 2(2):63–67. [PubMed: 4830514]
9. Riede G. Development of the lundia pro dialyzer. Blood Purif. 1986; 4(1-3):13–22. doi: 10.1159/000169422. [PubMed: 3730156]
10. Tuhy AR, Anderson EK, Jovanovic GN. Urea separation in flat-plate microchannel hemodialyzer; experiment and modeling. Biomed Microdevices. 2012; 14(3):595–602. doi: 10.1007/s10544-012-9638-7. [PubMed: 22374475]
11. Twardowski ZJ. History of hemodialyzers' designs. Hemodial Int. 2008; 12(2):173–210. doi: 10.1111/j.1542-4758.2008.00253.x. [PubMed: 18394051]
12. Fissell WH, Dubnisheva A, Eldridge AN, Fleischman AJ, Zydney AL, Roy S. High-performance silicon nanopore hemofiltration membranes. J Memb Sci. 2009; 326(1):58–63. doi: 10.1016/j.memsci.2008.09.039. [PubMed: 20054402]
13. Ahmadi M, Gorbet M, Yeow JTW. In vitro clearance and hemocompatibility assessment of ultrathin nanoporous silicon membranes for hemodialysis applications using human whole blood. Blood Purif. 2013; 35(4):305–313. doi: 10.1159/000350613. [PubMed: 23920150]
14. Johnson DG, Khire TS, Lyubarskaya YL, et al. Ultrathin silicon membranes for wearable dialysis. Advances in Chronic Kidney Disease. 2013; 20(6):508–515. doi: 10.1053/j.ackd.2013.08.001. [PubMed: 24206603]
15. Kanani DM, Fissell WH, Roy S, Dubnisheva A, Fleischman A, Zydney AL. Permeability - selectivity analysis for ultrafiltration: Effect of pore geometry. J Memb Sci. 2010; 349(1-2):405. doi: 10.1016/j.memsci.2009.12.003. [PubMed: 20161691]
16. Muthusubramaniam L, Lowe R, Fissell WH, et al. Hemocompatibility of silicon-based substrates for biomedical implant applications. Ann Biomed Eng. 2011; 39(4):1296–1305. doi: 10.1007/s10439-011-0256-y. [PubMed: 21287275]
17. Olorunsola OG, Kim SH, Chang R, et al. Imaging assessment of a portable hemodialysis device: Detection of possible failure modes and monitoring of functional performance. Medical instrumentation (Luton, England). 2014; 2(2) 10.7243/2052-6962-2-2. doi: 10.7243/2052-6962-2-2.
18. Rasband, WS. [Accessed 2/18, 2014] Image J, U.S. national institutes of health, bethesda, maryland, USA. http://imagej.nih.gov/ij/
19. Bankhead, P. [Accessed 01/17, 2014] Analyzing fluorescence microscopy images with ImageJ. http://imagej.nih.gov/ij/docs/examples/
20. Schneider CA, Rasband WS, Eliceiri KW. NIH image to ImageJ: 25 years of image analysis. Nature Methods. 2012; 9(7):671–675. doi: 10.1038/nmeth.2089. [PubMed: 22930834]
21. Hemodialysis Adequacy 2006 Work Group. Clinical practice guidelines for hemodialysis adequacy, update 2006. Am J Kidney Dis. 2006; 48(Suppl 1):S2–90. [PubMed: 16813990]

Author Manuscript Author Manuscript Author Manuscript Author Manuscript

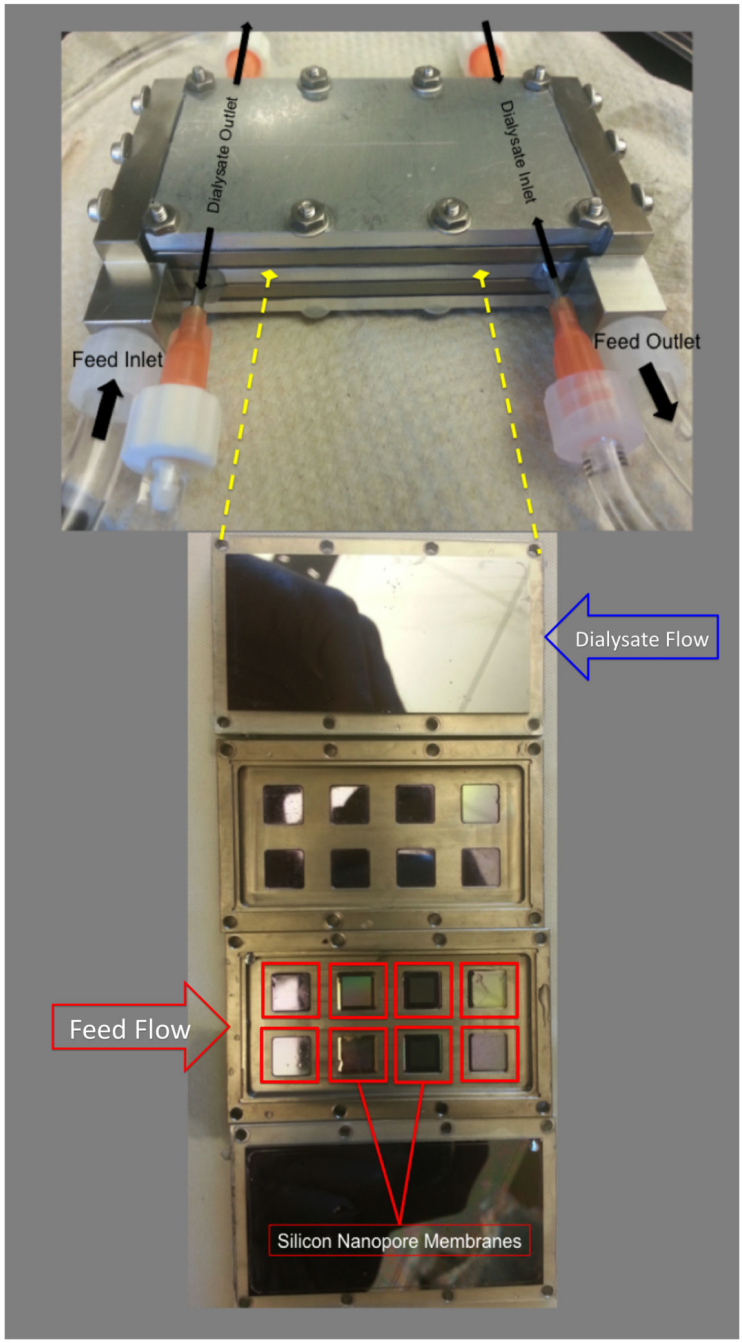


**Figure 1.**

Assembled parallel plate array with blood inlet/outlet and counter current dialysate inlet/outlet. The stacked parallel plates are shown below with 8 silicon nanopore membranes outlined in red and 8 solid silicon chips (not outlined). The arrows indicate the flow inlet and direction of the feed and dialysate, respectively.

Author Manuscript
Author Manuscript
Author Manuscript
Author Manuscript



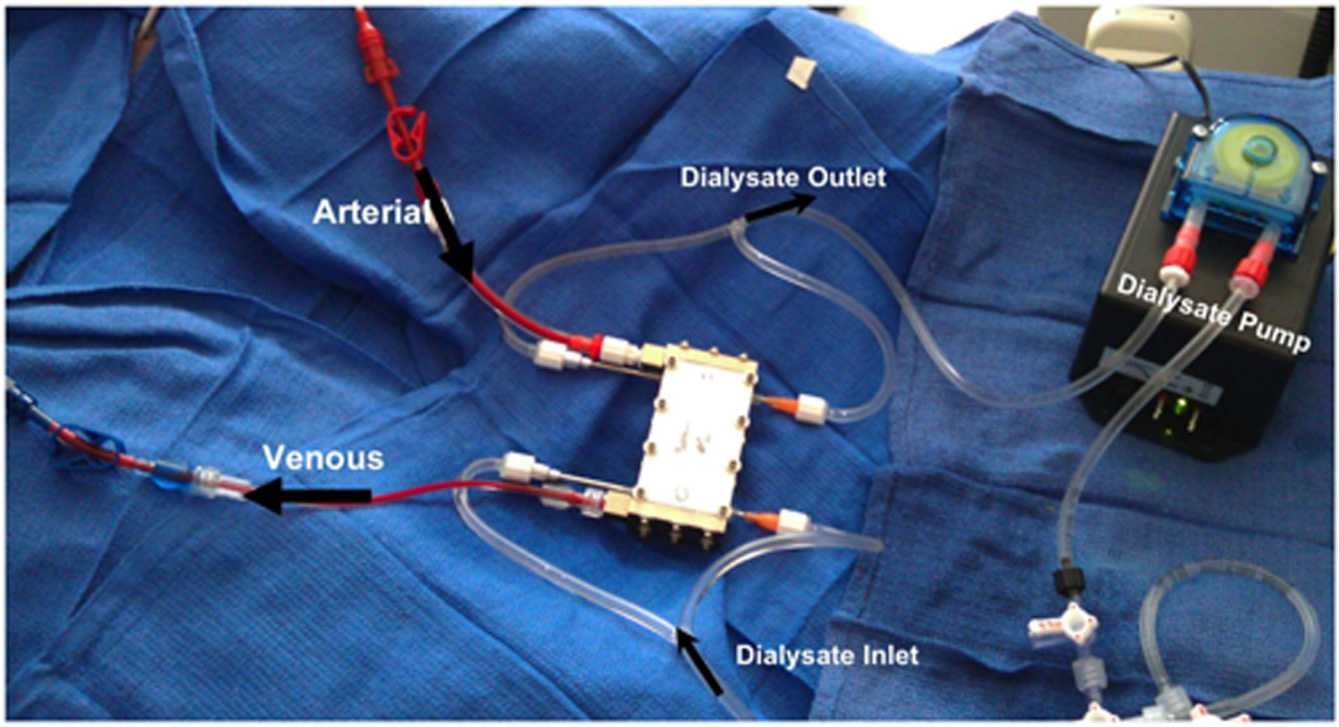


**Figure 2a.**

Ex vivo porcine experiment. Arterial and venous inlet and outlet labeled with arrows indicating the direction of flow. Dialysate inlet and outlet with arrows indicating the counter-current flow of dialysate.

Author Manuscript Author Manuscript Author Manuscript Author Manuscript

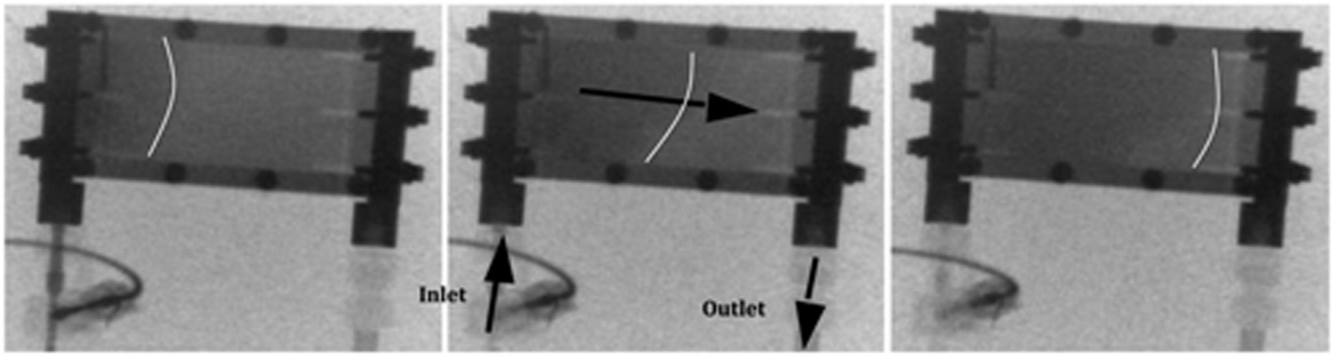


**Figure 2b.**

Fluoroscopy time-lapse images (Top down view). Cine images were obtained following a 90s dynamic infusion of contrast. Representative images at the start, middle and end of contrast infusion are shown. White lines are labeled to indicate contrast front. Black arrows show direction for blood flow.

Author Manuscript Author Manuscript Author Manuscript Author Manuscript

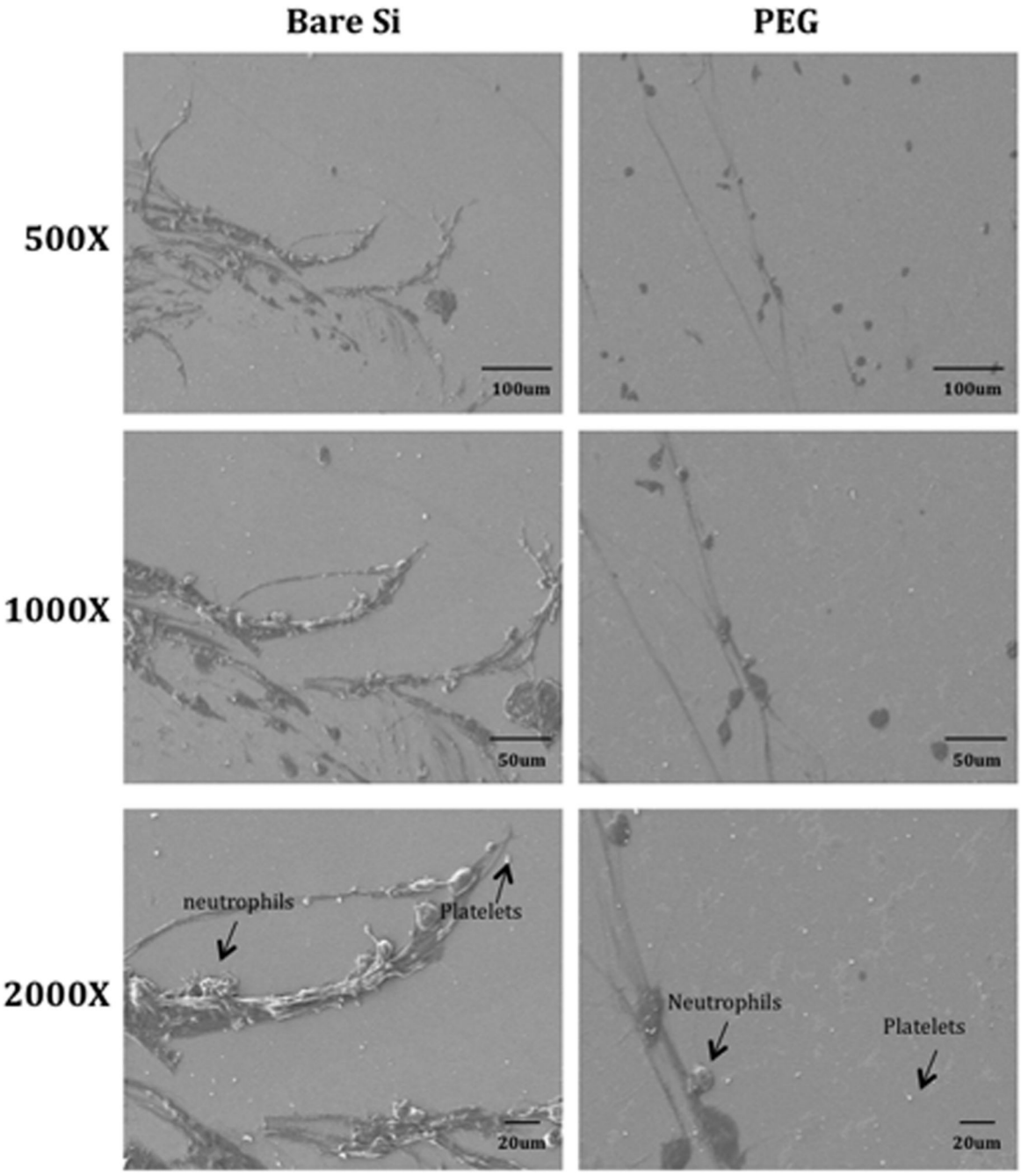


**Figure 3.**

SEM images showing neutrophils (average sizes: 12-17μm), platelets (average sizes: 1-6 μm) and red blood cells (average sizes: 8-10 μm) adhesion on bare silicon (Si) and PEG-coated substrates. Thread like structures represents fibrin formation.

Author Manuscript Author Manuscript Author Manuscript Author Manuscript

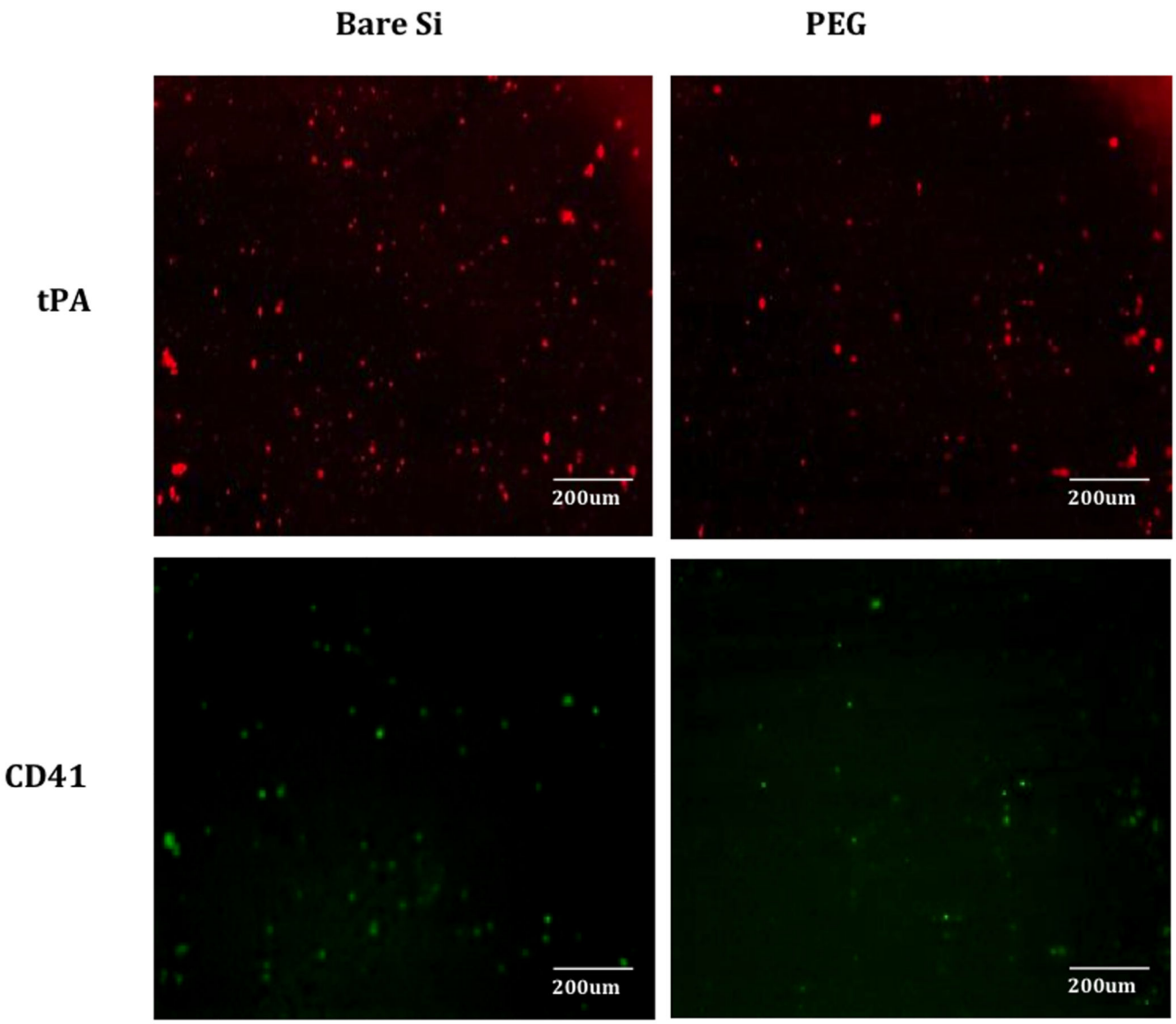


**Figure 4.**

Representative images showing platelet adhesion and blood clots as visualized by immunofluorescence staining for t-PA (in red, blood clotting marker) and CD41 (in green, platelet marker) and on varying substrates after porcine study; bare silicon (Si), PEG-coated substrates.

Author Manuscript

Author Manuscript

Author Manuscript

Author Manuscript

## Table 1

Clearance (K) for creatinine, urea, and phosphorus in albumin solution and whole blood.

| Diffusive Clearance (ml/min/m$^2$) | | |
|---|---|---|
| | **Parallel Plate Array (Albumin Solution)** | **Parallel Plate Array (Whole Blood)** |
| **Creatinine** | 84.0 ± 15.3 | 127.6 ± 14.0 |
| **Urea** | 115.2 ± 17.8 | 117.1 ± 16.0 |
| **$PO_4$** | 64.2 ± 14.7 | 56.5 ± 9.6 |

Author Manuscript

Author Manuscript

Author Manuscript

Author Manuscript

## Table 2

Urea clearance (K) for commercial hollow-fiber dialyzers normalized to surface area clinical blood flow rates ($Q_b$) and dialysate flow rates ($Q_d$).

| | Surface Area ($m^2$) | K (ml/min/$m^2$) $Q_b$= 200ml/min $Q_d$= 500ml/min | K (ml/min/$m^2$) $Q_b$= 400ml/min $Q_d$= 500ml/min |
|---|---|---|---|
| **Fresenius Optiflux F160NR** | 1.5 | 129 | 205 |
| **Gambro Polyflux Revaclear** | 1.4 | 140 | 229 |
| **Asahi APS-650** | 1.3 | 143 | 210 |